

ORC6 acts as an effective prognostic predictor for non-small cell lung cancer and is closely associated with tumor progression

LETIAN CHEN^{1*}, DONGDONG ZHANG^{2*}, YUJUAN CHEN^{1*}, HUILAN ZHU¹,
ZHIPENG LIU¹, ZHIPING YU¹ and JUNPING XIE¹

Departments of ¹Pulmonary and Critical Care Medicine and ²General Surgery,
The Second Affiliated Hospital of Nanchang University, Nanchang, Jiangxi 330000, P.R. China

Received September 26, 2023; Accepted December 7, 2023

DOI: 10.3892/ol.2024.14229

Abstract. Origin recognition complexes (ORCs) are vital in the control of DNA replication and the progression of the cell cycle, however the precise function and mechanism of ORC6 in non-small cell lung cancer (NSCLC) is still not well understood. The present study used bioinformatics methods to assess the predictive significance of ORC6 expression in NSCLC. Moreover, the expression of ORC6 was further evaluated using reverse transcription-quantitative PCR and western blotting, and its functional significance in lung cancer was assessed via knockdown experiments using small interfering RNA. A significant association was demonstrated between the expression of ORC6 and the clinical features of NSCLC. In particular, elevated levels of ORC6 were significantly strongly correlated with an unfavorable prognosis. Multivariate analysis demonstrated that increased ORC6 expression independently contributed to the risk of overall survival (HR 1.304; P=0.015) in individuals diagnosed with NSCLC. Analysis of Kaplan-Meier plots demonstrated that ORC6 expression served as a valuable indicator for diagnosing and predicting the prognosis of NSCLC. Moreover, *in vitro* studies demonstrated that modified ORC6 expression had a significant impact on the proliferation, migration and metastasis of NSCLC cells. NSCLC cell lines (H1299 and mH1650) exhibited markedly higher ORC6 expression than normal lung cell lines. The results of the present study indicated a strong association between the expression of ORC6 and the clinicopathological characteristics of NSCLC, which suggested its potential as a reliable biomarker for predicting

NSCLC. Furthermore, ORC6 may have important therapeutic implications in the management of NSCLC.

Introduction

Lung cancer is one of the primary factors contributing to mortalities caused by cancer. Every year, there are an estimated 2 million new cases and 1.76 million mortalities. The majority of lung cancer cases are attributed to non-small cell lung cancer (NSCLC), accounting for ~80% of all diagnosed lung cancer cases (1). Over the past few years, the emergence of immune checkpoint inhibitors (ICIs) has brought significant advancements in cancer immunotherapy. The management of NSCLC has undergone a complete transformation and demonstrates long-lasting effectiveness in ~20% of cases. However, the absence of dependable prognostic indicators for immunotherapy prevents numerous patients from reaping the advantages of this therapy (2).

In 2016, two studies, namely OAK study involving atezolizumab, and the KEYNOTE-010 study involving pembrolizumab, reported a notable association between the expression of programmed death-ligand 1 (PD-L1) in tumor tissue samples and the effectiveness of immunotherapy, specifically in terms of enhanced survival and response rates (3,4). Furthermore, subsequent retrospective studies have further validated the significance of PD-L1 as a predictive biomarker for the efficacy of ICIs (5,6). However, ICIs may still elicit a response in certain patients who exhibit low or negative levels of PD-L1 expression and the diversity and fluctuation over time of PD-L1 expression (7) emphasizes the idea that relying solely on PD-L1 may not be sufficient to identify the particular patients group that would benefit from NSCLC immunotherapy.

The effectiveness of lung cancer therapy appears to depend on the existence of biomarkers (8). As a result, there is a pressing need to identify new and efficient prognostic biomarkers for NSCLC as well as novel therapeutic targets.

The origin recognition complex (ORC) consists of six subunits: ORC1, ORC2, ORC3, ORC4, ORC5 and ORC6, which form a heterohexameric protein complex. ORC acts as a crucial ATPase in eukaryotes, creating a hexamer resembling a ring that attaches to the replication origin. This attachment helps in the loading of minichromosome maintenance 2-7 and

Correspondence to: Professor Junping Xie, Department of Respiratory and Critical Care Medicine, The Second Affiliated Hospital of Nanchang University, 1 Minde Road, Donghu, Nanchang, Jiangxi 330000, P.R. China
E-mail: junpingxie@sina.com

*Contributed equally

Key words: origin recognition complex 6, non-small cell lung cancer, biomarker, prognosis

the initiation of DNA replication (9). In addition, ORC serves a role in determining transcription domains (10).

ORC6, an essential component of the ORC in human cells, serves a vital foundation for the initial assembly of the ORC, that is required for DNA replication. The participation of ORC in DNA replication in yeast and fruit flies have been reported in previous studies (11,12). Despite serving different functions across different species, ORC6 remains indispensable for DNA replication in all studied organisms (13). Human ORC6 displays similarity to transcription factor II B and is able to directly bind to DNA (14). Long-term depletion of ORC6 has been previously reported to reduce cell proliferation and enhance cell mortality, underscoring its importance as a gene that coordinates chromosome replication and segregation with cytokinesis (15). Furthermore, increasing evidence suggests that an imbalance of ORC6 is associated with the emergence of diverse types of human malignancies, such as hepatocellular carcinoma (16), renal cancer (17), mammary carcinoma (18), colon cancer (19), prostatic carcinoma (20) and uterine cancer (21). However, limited information is available regarding the precise function and mechanisms of ORC6 in NSCLC. Thus, the present study assessed the physiological roles of ORC6 in NSCLC and to elucidate its possible mechanisms.

Materials and methods

Bioinformatics analysis. The present study analyzed a NSCLC dataset [TCGA Lung Adenocarcinoma (LUAD)] consisting of 541 collected tumor tissue samples and 59 normal tissue samples from The Cancer Genome Atlas (TCGA; <https://tcga-data.nci.nih.gov/tcga/>) (22). Certain tumor tissue samples were associated with their paired normal tissues, while other tumor tissues are not associated with adjacent normal tissues. A bioinformatics analysis was performed on the aforementioned TCGA dataset to evaluate the association between the expression of ORC6 and the prognosis of patients with NSCLC. The Wilcoxon rank-sum test and logistic regression analysis were used to assess the association between ORC6 expression and clinical features of patients with NSCLC. Moreover, Kaplan-Meier and Cox regression analyses were used to evaluate the influence of ORC6 expression levels on overall survival (OS). To visualize the association between the expression of the ORC6 gene and the risk of NSCLC, a forest plot was created. Furthermore, the present study used the survival (version 3.2-13; Comprehensive R Archive Network) and survminer (version 0.4.9; Comprehensive R Archive Network) packages of R 4.0.5 (<http://www.r-project.org/>) (23) for the analysis of patient survival and prognosis. Enrichment analysis of DEGs was performed using the KEGG and GO databases. The dataset named TCGA Lung Adenocarcinoma (LUAD) was selected and the limma package in R 4.0.5 (version 3.48.3; <http://www.bioconductor.org>) (24) was used to identify genes that were differentially expressed. Samples were categorized according to the median expression of ORC6, and DEGs were selected based on the conditions of log fold-change >1 and adjusted $P < 0.05$. CIBERSORT (<https://cibersort.stanford.edu/>) was used to calculate the relative proportions of 22 infiltrating immune cells in each patient (25). The single-sample gene set enrichment analysis

(ssGSEA) algorithm was performed using the GSVA R package (version 1.38.1; <http://www.bioconductor.org>) (26).

Cell culture and transient transfection. Cancer cell lines (A549, PC-9, H1299 and H1650) and normal cell lines (BEAS-2B) were purchased from Procell Life Science & Technology Co., Ltd. PC9, H1299, and H1650 cells were cultured in RPMI1640 medium (Gibco; Thermo Fisher Scientific, Inc.), while A549 and BEAS-2B cells were cultured in DMEM (Gibco; Thermo Fisher Scientific, Inc.). All media were supplemented with 10% fetal bovine serum (FBS; Gibco; Thermo Fisher Scientific, Inc.), 100 $\mu\text{g}/\text{ml}$ streptomycin, and 100 U/ml penicillin sodium (Beijing Solarbio Science & Technology Co., Ltd.). The cells were cultured in an incubator at 37°C and 5% CO_2 . To assess the impact of ORC6 on lung cancer cells, the H1299 and H1650 lung cancer cell lines were subjected to RNA interference to transiently decrease the expression of the ORC6 gene. Transfection with small interfering (si)RNA (20 pmol/ μl) was performed using Lipofectamine[®] 3000 (Invitrogen; Thermo Fisher Scientific, Inc.). SiRNA (5 μl) and Lipofectamine[®] 3000 (Invitrogen; Thermo Fisher Scientific, Inc.; 5 μl) was diluted in serum-free culture medium. The diluted Lipofectamine[®] 3000 was added to the diluted siRNA and incubated at room temperature for 20 min before being added to the cell suspension. Subsequently, the mixture was incubated at 37°C for 6 h to complete transfection. Then, the medium in each well was replaced with RPMI1640 medium containing 10% FBS. Following a period of 48 h, successful transfection was validated using western blotting as detailed below and 48 h after transfection, the cells were used for subsequent experiments. The sequences of the siRNAs from General Biotech (Anhui) Co., Ltd.) were as follows: siORC6-1, 5'-GGCUUAUUUAAU UAAACUU-3'; siORC6-2, 5'-GCUUCAAGAAUACUAAAA A-3'; siORC6-3, 5'-GAAUGGAAAAGAAAAUUU-3'; and si-negative control (NC), 5'-UUCUCCGACGUGUCACGU-3'.

RNA extraction and reverse transcription(RT)-quantitative (q)PCR. After extracting total RNA from A549, PC-9, H1299, H1650 and BEAS-2B cells using TRIzol[®] reagent (Thermo Fisher Scientific, Inc.), a NanoDrop[™] 2000 spectrophotometer (NanoDrop Technologies; Thermo Fisher Scientific, Inc.) was used to measure the concentration and purity of total RNA. Subsequently, cDNA was synthesized using the PrimeScript RT-PCR Kit (Takara Bio, Inc.) at 37°C for 15 min and 85°C for 5 sec. qPCR was performed with TB Green Premix Ex Taq II (cat. no. RR820A; Takara Biotechnology Co., Ltd.) on a CFX96 real-time PCR detection system (Bio-Rad Laboratories, Inc.). The reaction conditions were 94.0°C for 30 sec, followed by 94.0°C for 4 sec, 58.0°C for 15 sec and 72°C for 15 sec for a total of 40 cycles. The $2^{-\Delta\Delta\text{C}_q}$ method (27) was used to calculate relative expression, and GAPDH served as the endogenous control for normalization. The primers used were purchased from Sangon Biotech Co, Ltd. with sequences as follows: GAPDH forward (F), 5'-AAAGCATCACCCGG AGGAGAA-3' and reverse (R), 5'-AAGGAAATGAATGGG CAGCCG-3'; and ORC6 F, 5'-ACAAGGAGACATATCAGA GCTGT-3' and R, 5'-AGTGGCCTGGATAAGTCAAGAT-3'.

Western blotting. A total of 5×10^5 transfected H1299 and H1650 cells (with si-NC as the negative control), were

collected following two washes with PBS, via centrifugation at 10,000 x g for 10 min at 4°C. Subsequently, the supernatant was discarded, using radioimmunoprecipitation assay (RIPA) lysis buffer (Shanghai Beibo Biotechnology Co., Ltd.) and the protein concentration was measured using a BCA protein assay kit (Beyotime Institute of Biotechnology). After adding 1% mercaptoethanol, denaturation was performed at a 100°C for 10 min, and the protein samples (20 µg/lane) underwent SDS-PAGE on a 10% gel, followed by transfer onto nitrocellulose membranes. To block the membranes, they were incubated with 5% non-fat milk at 25°C for 2 h. The membranes were incubated overnight at 4°C with anti-ORC6 polyclonal antibodies (1:1,000; cat. no. A5426; ABclonal Biotech Co., Ltd.) and anti-β-actin monoclonal antibodies (1:3,000; cat. no. ab8226; Abcam). Following three washes with TBS-Tween 20 (TBST; 0.1% Tween) for 10 min each, the membrane was incubated with horseradish peroxidase-conjugated secondary antibodies (1:10,000; cat. nos. SA00001-1 and SA00001-2; Proteintech Group, Inc.) at room temperature for 1 h. Subsequently, the membranes were washed with TBST and incubated with ECL chemiluminescence reagent (Beyotime Institute of Biotechnology). The protein bands were then analyzed using Image Lab analysis software (version 4.0; Bio-Rad Laboratories, Inc.). The experiment was performed in triplicate.

Wound healing assays. H1299 and H1650 cells, transfected with 2x10⁵ cells each, were evenly distributed in 6-well culture dishes and cultured until they reached ~90% confluency. A 200-µl pipette tip was used to generate a scratch on the culture plate. Subsequently, the cells were 3 times washed with PBS, added to a serum-free RPMI1640 medium and placed in an incubator at 37°C. Images of the scratch were captured under an light microscope at 0 and 24 h to observe the movement of cells and the process of wound healing. ImageJ (version 1.8.0; National Institutes of Health) was used to calculate the % wound healing.

Transwell migration assays. To perform the Transwell migration assay, H1299 and H1650 cells were resuspended in RPMI1640 medium (Gibco; Thermo Fisher Scientific, Inc.) without serum at a concentration of 2x10⁴ cells per Transwell plate. At the same time, complete medium with 15% FBS (Gibco; Thermo Fisher Scientific, Inc.) was added to the lower chamber. Following incubation for 24 h at 37°C, cells that had moved to the lower chamber were treated with 3% paraformaldehyde for fixation at 25°C for 30 min then stained using crystal violet, cells were imaged and enumerated using an inverted microscope and ImageJ (version 1.8.0; National Institutes of Health).

Cell Counting Kit-8 (CCK-8) assay. Cells were added to a 96-well plate at a density of 3,000 cells per well. Cell proliferation rate [optical density (OD) value] was measured using CCK-8 reagent (Dojindo Laboratories, Inc.) at 0, 24, 48 and 72 h (incubated at 37°C for 2 h).

Analysis of apoptosis. H1299 and H1650 cells were resuspended in binding buffer (Beyotime Institute of Biotechnology) and cell concentration was adjusted to 1x10⁶ cells/ml. In each

group, 100 µl cell suspension was mixed with 5 µl annexin V/FITC staining solution and 10 µl propidium iodide staining solution (20 µg/ml; Beyotime Institute of Biotechnology), followed by incubation at room temperature for 15 min in the dark. Next, a flow cytometer (FACScan; BD Biosciences) was used to examine cell apoptosis and the results were analyzed using FlowJo (version 10; FlowJo LLC).

Statistical analysis. ORC6 expression levels in patients with NSCLC were visualized using scatter plots and box plots. Patients were categorized into groups based on gene expression using median ORC6 expression as the cutoff value. The association between clinical characteristics of NSCLC and ORC6 expression was assessed using the Wilcoxon rank-sum test and logistic regression analyses. The log-rank test was used to determine significance. Potential prognostic factors were identified using univariate and multivariate Cox analyses. Spearman's rank or Pearson's correlation coefficient were performed to assess correlations between the groups.

Data analysis was performed using GraphPad Prism v7.0 software (Dotmatics). Differences between two groups were analyzed using paired or independent t-tests as appropriate. One-way analysis of variance, followed by Dunnett's post-hoc test, and the Kruskal-Wallis test, followed by Dunn's post-hoc test, were used for comparisons between multiple groups. All quantitative experiments were repeated three times and the results are reported as mean ± standard deviation. All statistical tests were two-sided. P<0.05 was considered to indicate a statistically significant difference.

Results

Relative expression of the ORC family in NSCLC. To assess the expression patterns of the ORC family during the progression of NSCLC, mRNA expression data for 6 members of the ORC family were extracted from the TCGA database. The differences in expression of each family member between NSCLC tissues and the corresponding normal tissues were analyzed. Compared with normal tissues, ORC2 expression was notably decreased in NSCLC tissues, whilst the expression levels of ORC3, ORC4 and ORC5 were markedly elevated but without statistical significance. Significant increases in the expression of ORC1 and ORC6 were observed in NSCLC tissues, compared with that in normal tissues (Fig. 1A-F).

Prognostic significance of ORC1 and ORC6 in NSCLC. Kaplan-Meier analysis revealed that the expression level of ORC1 was not associated with OS (Fig. 1G). However, a significantly higher expression of ORC6 was associated with a worse OS (Fig. 1H). Therefore, the present study focused on ORC6 to evaluate its involvement in the progression of NSCLC.

Relative expression of ORC6 in NSCLC. The expression of ORC6 at mRNA level in various cancers was calculated by using Tumor Immune Estimation Resource (TIMER 2.0; <http://timer.cistrome.org/>) (28). The results of the present study showed that ORC6 was significantly associated with LUAD, LUSC, PCPG, PRAD, READ, SKCM, STAD, THCA, UCEC, LIHC, KIRP, KIRC, KICH, HNSC, HNSC-HPV, GBM, ESCA, COAD, CHOL, CESC, BRCA and BLCA (Fig. 2A).

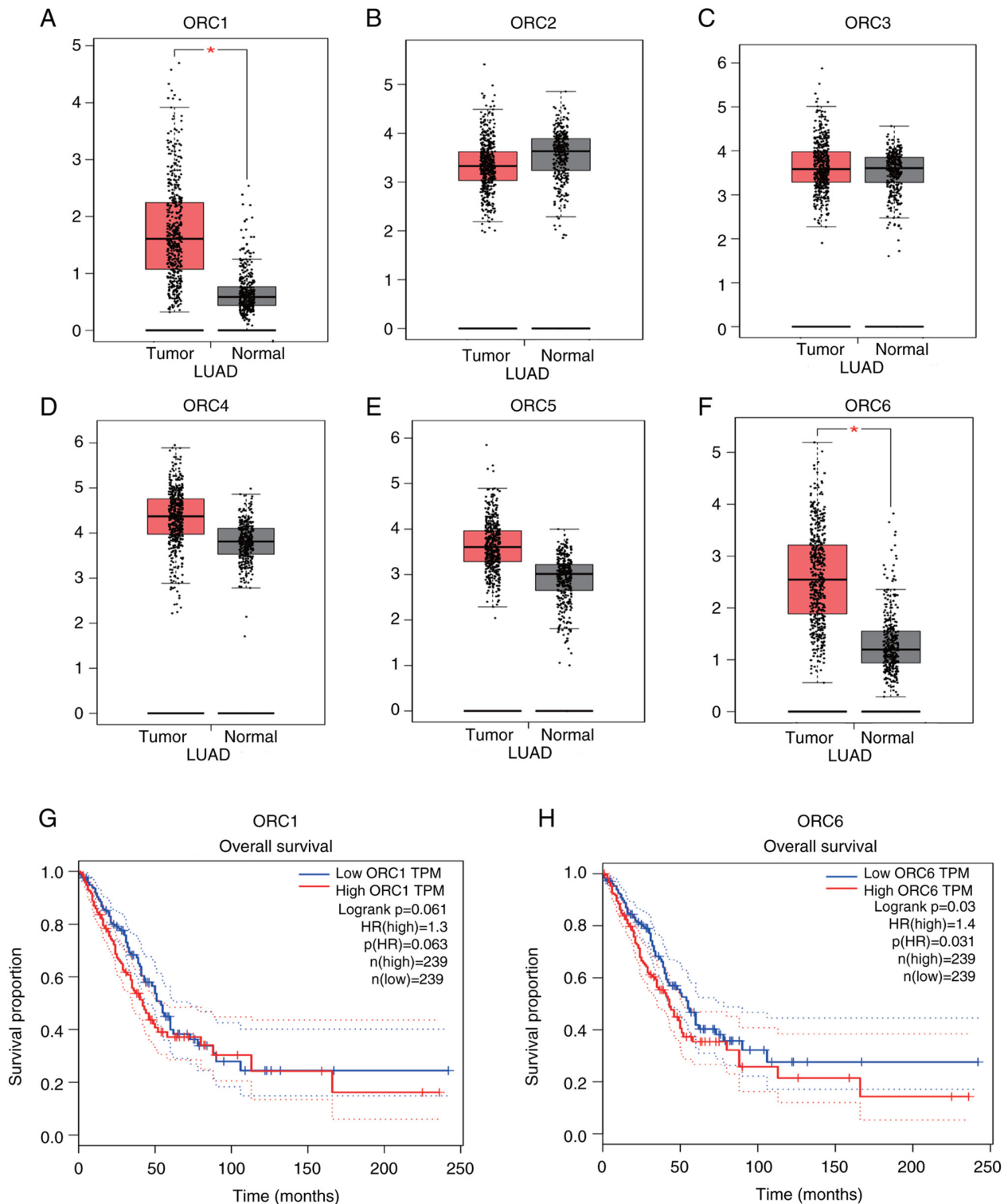


Figure 1. Relative expression of the ORC family in NSCLC and its impact on prognosis. mRNA expression data for the 6 members of the ORC family in tumor: (A) ORC1, (B) ORC2, (C) ORC3, (D) ORC4, (E) ORC5 and (F) ORC6. Prognostic significance of (G) ORC1 and (H) ORC6 in NSCLC. * $P < 0.05$. ORC, origin recognition complex; LUAD, lung adenocarcinoma; TPM, transcripts per million.

Subsequently, the expression levels of ORC6 in NSCLC and normal lung tissues were analyzed using data from the TCGA database. The analysis revealed that the expression of ORC6 was significantly elevated in NSCLC tissues in comparison with normal lung tissues ($P < 0.001$; Fig. 2B). This outcome was further demonstrated when analyzing paired tissues ($P < 0.001$; Fig. 2C). These findings suggested that ORC6 may play a

crucial role in the development of cancer, providing essential clues for further investigations into its mechanistic role.

Relative expression of ORC6 in normal lung tissues. Transcription and clinical data for normal lung tissues were downloaded from the TCGA database. Clinical and transcriptome information were merged, and statistical analysis was

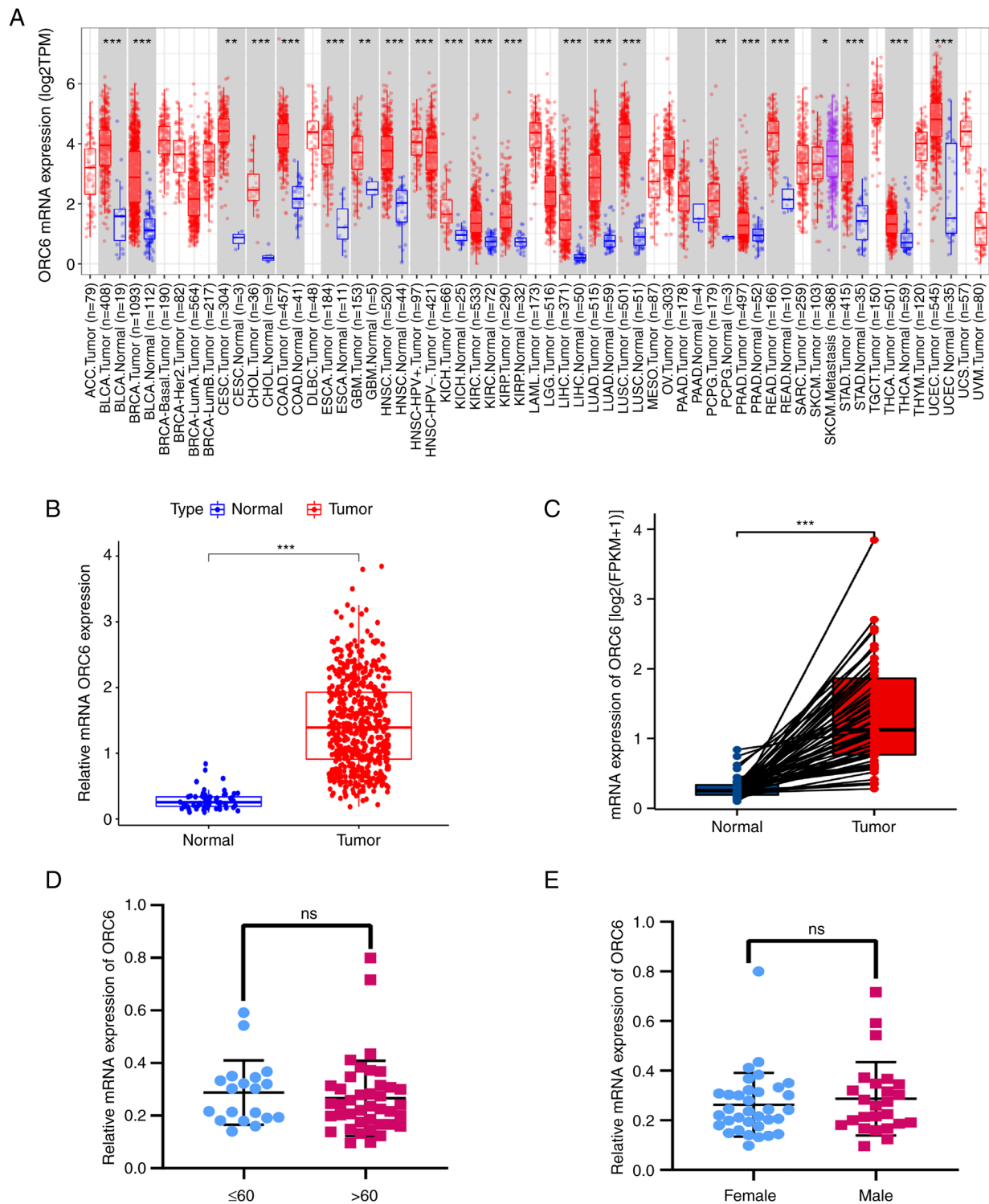


Figure 2. Pan-cancer expression of ORC6. (A) Expression of ORC6 across numerous cancers, demonstrated using data from the Tumor Immune Estimation Resource 2.0 database. Expression of ORC6 in (B) normal and tumor tissues and in (C) paired tissues. In normal lung tissues, there was no significant difference in the expression of ORC6 among individuals of different (D) age groups and (E) sexes. * $P < 0.05$, ** $P < 0.01$, *** $P < 0.001$. LUAD, Lung Adenocarcinoma; LUSC, Lung Squamous Cell Carcinoma; PCPG, Pheochromocytoma and Paraganglioma; PRAD, Prostate Adenocarcinoma; READ, Rectum Adenocarcinoma; SKCM, Skin Cutaneous Melanoma; STAD, Stomach Adenocarcinoma; THCA, Thyroid Carcinoma; UCEC, Uterine Corpus Endometrial Carcinoma; LIHC, Liver Hepatocellular Carcinoma; KIRP, Kidney Renal Papillary Cell Carcinoma; KIRC, Kidney Renal Clear Cell Carcinoma; KICH, Kidney Chromophobe; HNSC, Head and Neck Squamous Cell Carcinoma; HNSC-HPV, HPV-Positive Head and Neck Squamous Cell Carcinoma; GBM, Glioblastoma Multiforme; ESCA, Esophageal Adenocarcinoma; COAD, Colon Adenocarcinoma; CHOL, Cholangiocarcinoma; CESC, Cervical Squamous Cell Carcinoma; BRCA, Breast Invasive Carcinoma; BLCA, Bladder Urothelial Carcinoma; ORC, origin recognition complex; TPM, transcripts per million; ns, not significant; FPKM, Fragments Per Kilobase Million.

performed for age and sex. The results indicated that there is no significant difference in the expression of ORC6 among

individuals of different ages and sexes in normal lung tissues (Fig. 2D and E).

Clinical association of ORC6 in NSCLC. To evaluate the potential prognostic value of ORC6 upregulation in different patient subgroups based on OS in NSCLC, the Wilcoxon rank-sum test and the Kruskal-Wallis test (followed by Dunn's post-hoc test) were performed to assess the levels of ORC6 upregulation. The results indicated that the expression of ORC6 is associated with the following clinical characteristics: Age of ≤ 60 years (>60 vs. ≤ 60 years; Fig. 3A), male sex (male vs. female; Fig. 3B), metastasis (M) classification (M1 vs. M0; Fig. 3C), stage (stage I vs. IV, stage II vs. IV; Fig. 3E) and tumor (T) stage (T1 vs. T2; Fig. 3F). All these associations were statistically significant ($P < 0.05$). However, there was no statistically significant difference between ORC6 and node (N) stages (Fig. 3D). Considering that clinical tumor staging (T staging) and pathological TNM staging are prognostic factors for most cancers, the results indicated that patients in later T stages exhibited higher levels of ORC6 mRNA expression. Patients with higher pathological T and M stages also showed elevated levels of ORC6 expression. In conclusion, it can be inferred that ORC6 may contribute to an adverse prognosis in NSCLC.

Kaplan-Meier analysis of patient data from TCGA. Kaplan-Meier analysis was performed on the OS and progression-free survival patient data obtained from the TCGA database, using the R packages *survminer* and *survival*. The results indicated a significant association between ORC6 expression and NSCLC prognosis ($P < 0.05$; Fig. 4A and B). In addition, univariate Cox regression analysis revealed several factors that significantly impacted the prognosis of NSCLC, including stage, T and N stages, and ORC6 expression (Fig. 4C). Multivariate Cox regression analysis was performed and the results indicated that the prognosis of NSCLC was significantly influenced by stage and ORC6 expression (Fig. 4D). These analytical results confirmed the hypothesis of the present study.

KEGG and GO enrichment analysis of differentially expressed genes (DEGs). Enrichment analysis of DEGs was performed using the KEGG and GO databases. A total of 1,370 DEGs were obtained and their expression patterns were depicted using a heatmap (Fig. 5A) and volcano plot (Fig. 5B). To assess the possible biological roles of these DEGs, enrichment analyses using GO and KEGG datasets were performed. The results of KEGG enrichment analysis indicated numerous significantly enriched pathways, such as 'Neuroactive ligand-receptor interaction', 'Systemic lupus erythematosus' and 'Fanconi anemia pathway' (Fig. 5C). GO enrichment analysis demonstrated significant associations with different molecular functions and cellular components, such as 'organelle fission', 'nuclear division', 'chromosomes segregation', 'mitosis nuclear division', 'sister chromatid segregation', 'mitotic sister chromatid segregation', 'protein-DNA complex assembly', 'chromosomal region' and 'nuclear chromosome segregation' (Fig. 5D). These analyses revealed the significant involvement of these genes in multiple biological pathways and molecular functions, providing strong support for further understanding their roles in biological processes.

Gene correlation of ORC6 in lung cancer. To further assess the downstream roles of ORC6, Pearson's correlation coefficient

analysis was performed for ORC6 (Fig. 6A), which revealed strong correlations between ORC6 and numerous genes, including vasoactive intestinal peptide receptor 1 (VIPR1), indolethylamine n-methyltransferase (INMT), nuclear factor I/X (NFIX), Zw10 interacting kinetochore protein (ZWINT), cyclin-dependent kinase 1 (CDK1), baculoviral IAP repeat containing 5 (BIRC5), targeting protein for Xklp2 (TPX2), kinesin family member 4A (KIF4A), lamin B1 (LMNB1), FYVE and coiled-coil domain autophagy adaptor 1 (FYCO1) and HOP homeobox (HOPX). Among them, CDK1, TPX2, ZWINT, BIRC5 and KIF4A demonstrated the strongest significant associations with ORC6 (Fig. 6B-F). These results suggested that ORC6 may participate in the regulation of gene expression and activity, which could have important implications for the downstream functions of ORC6 in NSCLC. Further research is necessary to further elucidate the mechanisms and relevance of these associations in the biology of NSCLC.

ORC6 expression and tumor microenvironment (TME). Using CIBERSORT analysis, the presence of 22 different immune cell types in lung cancer was assessed. The present study demonstrated a correlation between ORC6 expression and 13 tumor-infiltrating immune cells (TICs). In total, six TICs, including activated memory CD4 T cells, M1 macrophages, M0 macrophages, and CD8 T, resting natural killer (NK) and follicular helper T cells, demonstrated a significant positive correlation with ORC6 expression (Fig. 7A). However, ORC6 expression demonstrated a significant negative correlation with seven TICs, namely CD4 memory resting T, resting mast and resting dendritic cells (DCs), monocytes, activated DCs, naive B cells and M2 macrophages. To further assess the patterns of immune cell infiltration at varying levels of ORC6 expression, the single-sample Gene Set Enrichment Analysis algorithm was used. The enrichment scores of naive B cells, memory resting CD4 T cells, monocytes, resting DCs, activated DCs and resting mast cells were significantly lower in the ORC6 high-expression group than in the ORC6 low-expression group. However, the ORC6 high-expression group demonstrated significantly higher enrichment scores for CD 8 T, memory-activated CD4 T, follicular helper T and resting NK cells, as well as for M0 and M1 macrophages (Fig. 7B). Further assessment using the TIMER 2.0 platform revealed significant negative correlations between the infiltration quantities of dormant mast and resting CD4 memory T cells with the level of expression of ORC6 (Fig. 7C and D). However, the levels of infiltration by M1 macrophages and activated CD4 memory T cells showed a significantly positive correlation with the expression of ORC6 (Fig. 7E and F). The expression of ORC6 in NSCLC is significantly correlated with various tumor-infiltrating immune cells, suggesting its potential key role in regulating immune cell infiltration.

Further assessment of the upregulation of ORC6 expression in NSCLC cells. To confirm the results obtained from the aforementioned analysis of data from public databases, RT-qPCR was performed using NSCLC cells. Analysis of the experimental results using one-way analysis of variance for comparisons between multiple groups, followed by Dunnett's post-hoc test, demonstrated that, compared with BEAS-2B

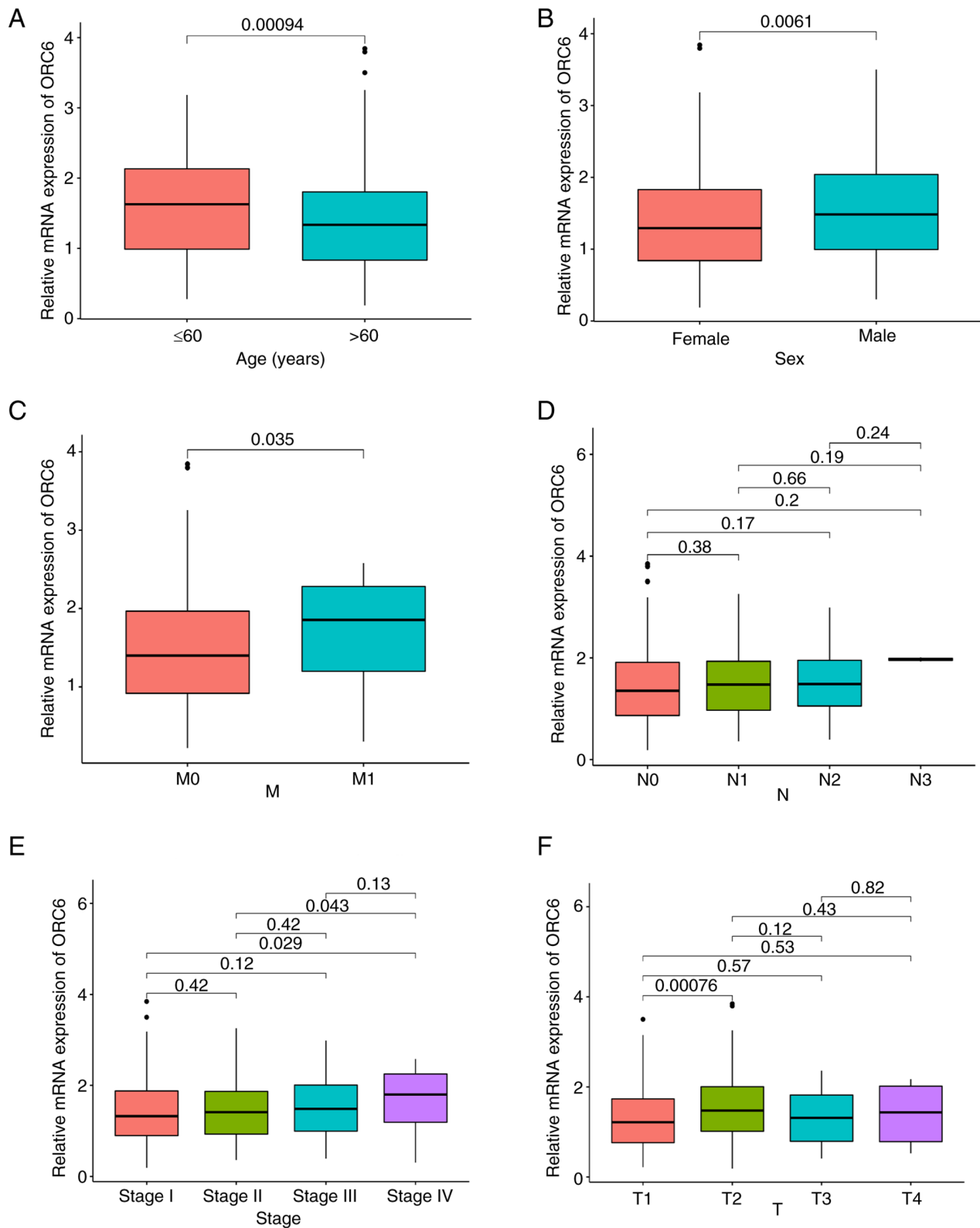


Figure 3. Associations between ORC6 expression and clinical factors. Association between ORC6 expression and (A) age and (B) sex. Variations in the mRNA expression of ORC6 across several clinical factors: (C) M stage, (D) N stage, (E) histological tumor grade and (F) T stage. ORC, origin recognition complex; T, tumor; N, node; M, metastasis.

cells, the mRNA levels of ORC6 significantly increased in H1299 and H1650 cells, whilst they significantly decreased in A549 and PC-9 cells (Fig. 8A). This may be attributed to genetic differences arising from the diverse origins of these cell lines, evolving in distinct environments (29).

Impairment of NSCLC malignancy upon ORC6 knock-down in vitro. To assess whether ORC6 could promote the malignant phenotype of NSCLC cells, three ORC6 siRNAs were transfected into H1299 and H1650 cells. After transfecting si-ORC6-3 into H1650 cells, there was a significant

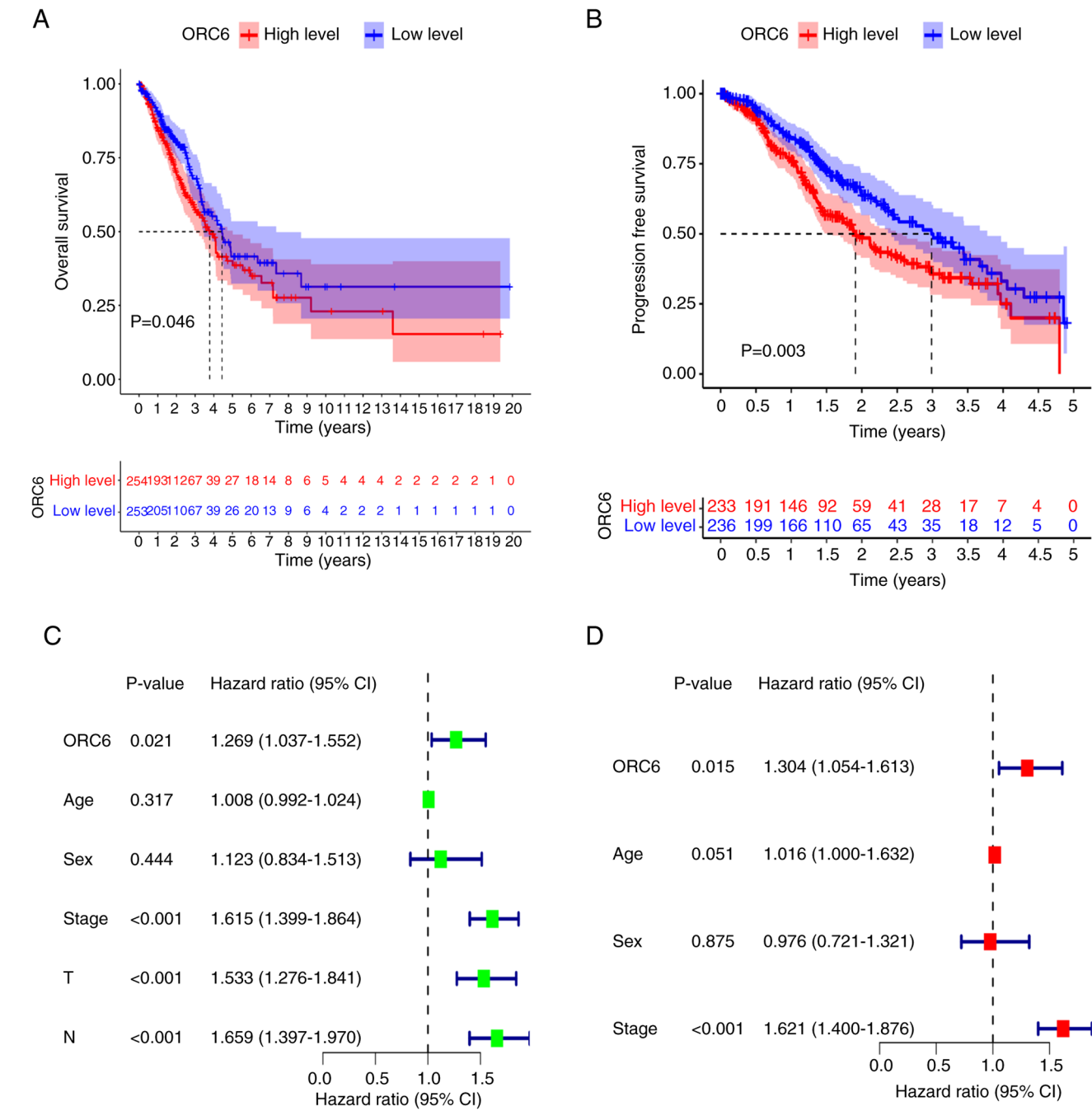


Figure 4. ORC6 Expression and Survival Analysis in Cancer Patients. Kaplan-Meier plots of (A) overall survival (B) and progression-free survival for patients in the high and low ORC6 expression groups. (C) Univariate and (D) multivariate Cox regression analysis. ORC, origin recognition complex; T, tumor; N, node.

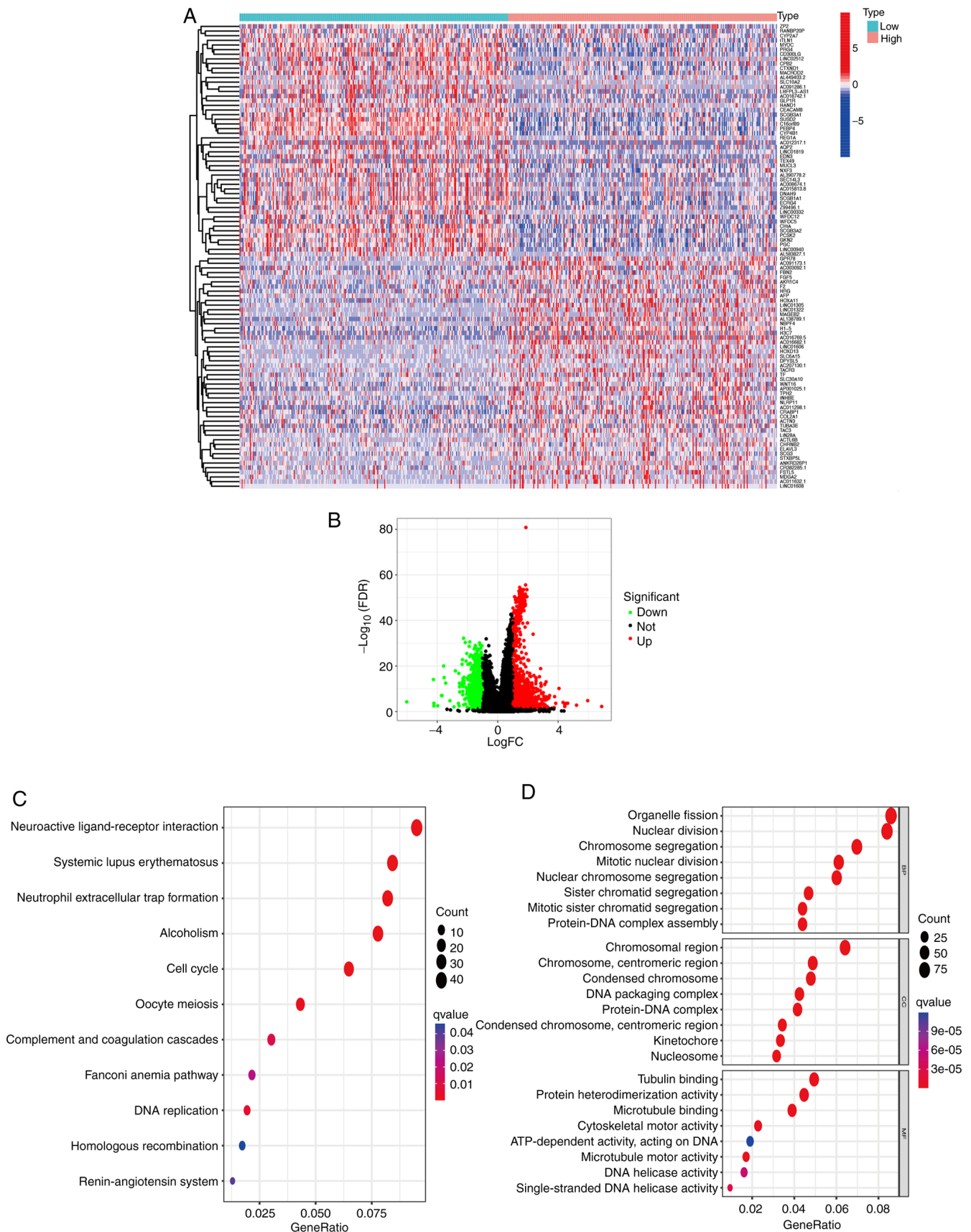
deterioration in cellular condition. Consequently, the present study opted to exclusively use si-ORC6-1 and si-ORC6-2 for the subsequent experiments in the H1650 cell line.

Western blotting confirmed the successful knockdown of ORC6 in both H1299 and H1650 cells (Fig. 8B and C). Wound healing assays indicated that the knockdown of ORC6 significantly inhibited the scratch wound healing ability of the cells, compared with that in si-NC-transfected cells (Fig. 8D and E). In Transwell assays, si-NC-transfected H1299 and H1650 cells demonstrated significantly stronger cell migration and invasion capabilities than the corresponding knocked-down cells (Figs. 8F and 9A). CCK-8 assays demonstrated that the knockdown of ORC6 significantly slowed down the proliferation of

H1299 cells at 48 and 72 h compared with si-NC-transfected cells. Similarly, at 24 and 72 h, the depletion of ORC6 significantly decelerated the proliferation of H1650 cells compared with si-NC-transfected cells (Fig. 9B and C). Cell apoptosis assays demonstrated that downregulation of ORC6 expression significantly promoted apoptosis in tumor cells (Fig. 9D and E). Overall, downregulation of ORC6 *in vitro* inhibited the malignancy of NSCLC.

Discussion

Among the ORC subunits, ORC6 is the smallest and least stable subunit, although it is a crucial component for the



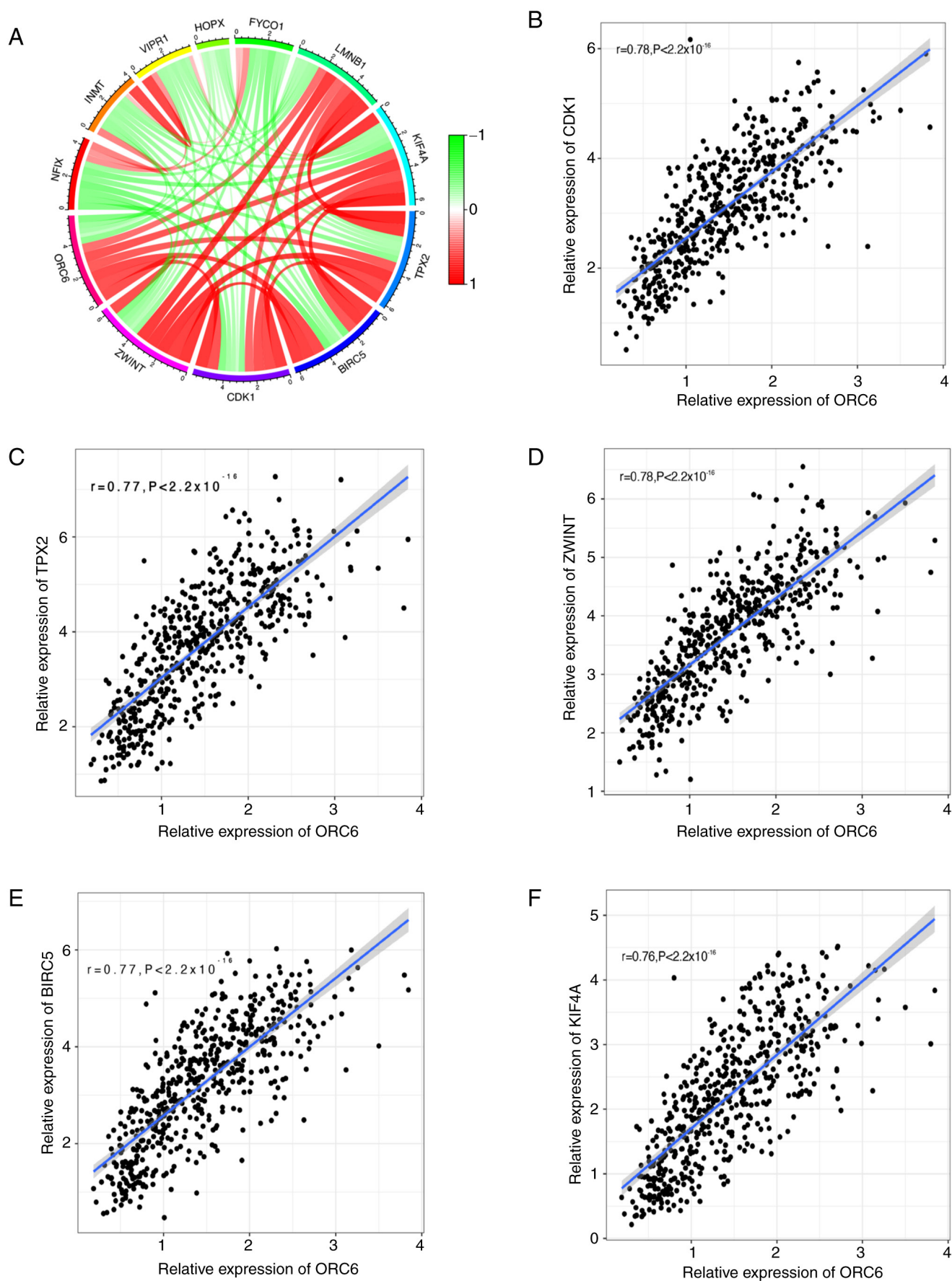


Figure 6. Gene correlation of ORC6. (A) Circos diagram illustrating the correlation between ORC6 and other genes in lung cancer; red shaded bars indicate a positive correlation between the connected genes, while the green shaded bars indicate a negative correlation between the connected genes. the genes demonstrating the highest correlation with ORC6: (B) CDK1, (C) TPX2, (D) ZWINT, (E), BIRC5 and (F) KIF4A. ORC, origin recognition complex. CDK1, cyclin-dependent kinase 1; TPX2, Targeting protein for Xklp2; ZWINT, ZW10 interacting kinetochore protein; BIRC5, baculoviral inhibitor of apoptosis repeat-containing 5; KIF4A, kinesin family member 4A.

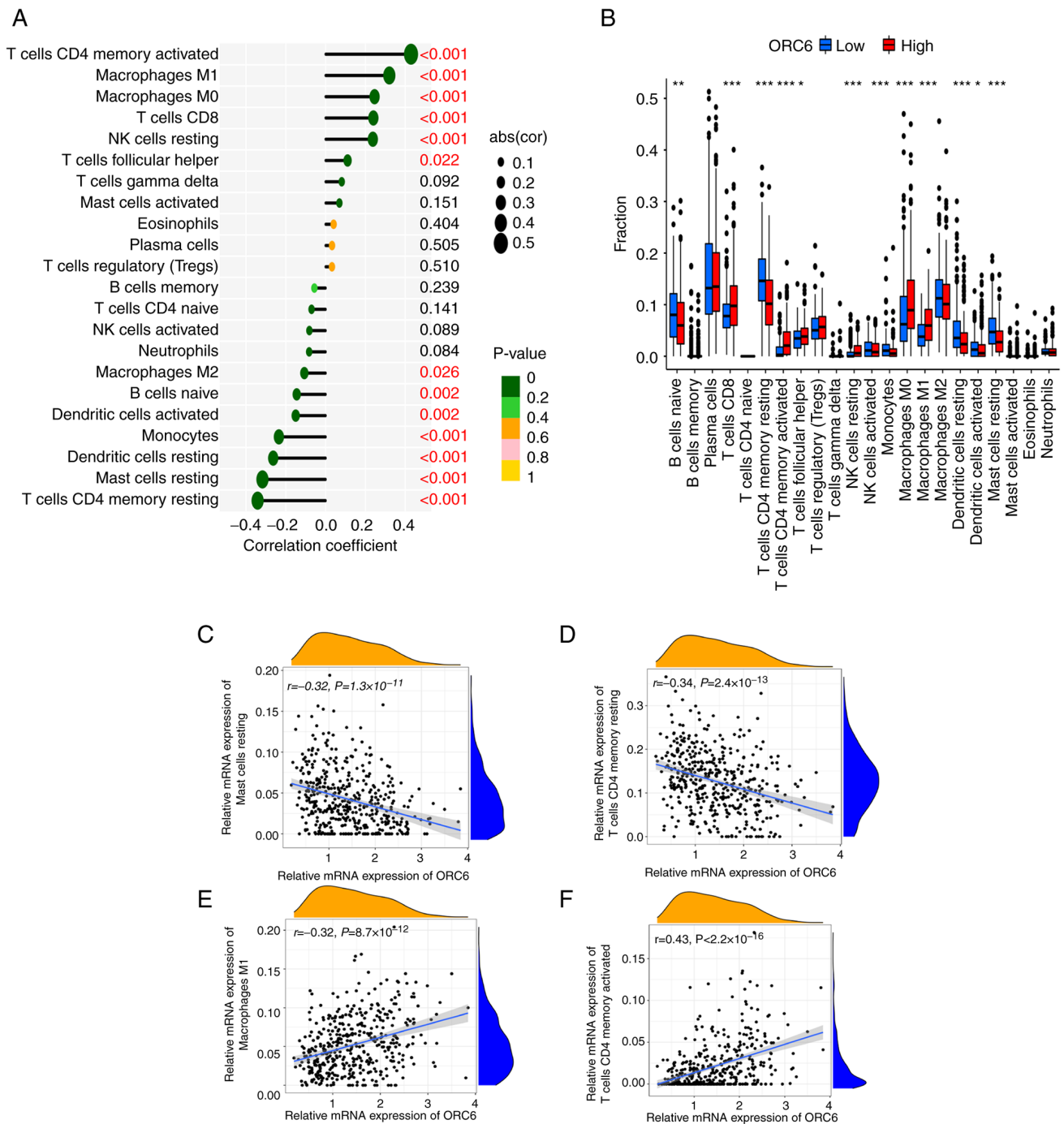


Figure 7. Correlation between the expression of ORC6 and the levels of immune infiltration in NSCLC. (A) Correlation between the expression of ORC6 and the proportionate infiltration of 22 different immune cell types in NSCLC. The size of the dots correspond to the Spearman's rank correlation coefficient values. (B) Differential enrichment scores for 22 immune cell types compared between patients with high and low levels of ORC6 expression. * $P < 0.05$; ** $P < 0.01$; *** $P < 0.001$. (C-F) The expression of ORC6 was strongly associated with the levels of (C) resting Mast cells, (D) resting memory T cells CD4, (E) M1 macrophages and (F) activated memory T cells CD4. ORC, origin recognition complex; NSCLC, non-small cell lung cancer; NK, natural killer.

survival of all species (30). The ORC surrounds DNA and uses its winged-helix domain to engage with the minichromosome maintenance 2-7 complex whilst loading the replication helicase (31). The presence of ORC6 is essential for DNA recognition in fruit flies, as the lack of ORC6 hinders the binding of ORC to DNA (32). Additionally, ORC6 is essential in the development of ORC companion proteins that aid in chromosomal attachment prior to DNA replication (33). Despite the well-established importance of ORC6 in the

prognosis of several tumors, the specific mechanisms linking ORC6 to NSCLC prognosis remain largely unexplored.

NSCLC represents 80-85% of all reported instances of lung cancer, resulting in >2 million new diagnoses annually on a global scale (34,35). Despite considerable progress in treatment approaches for NSCLC, the 5-year survival rate of patients is ~22%. (36). Moreover, NSCLC is a diverse and complex cancer type characterized by numerous genetic mutations (37). Thus, it is imperative to elucidate the possible

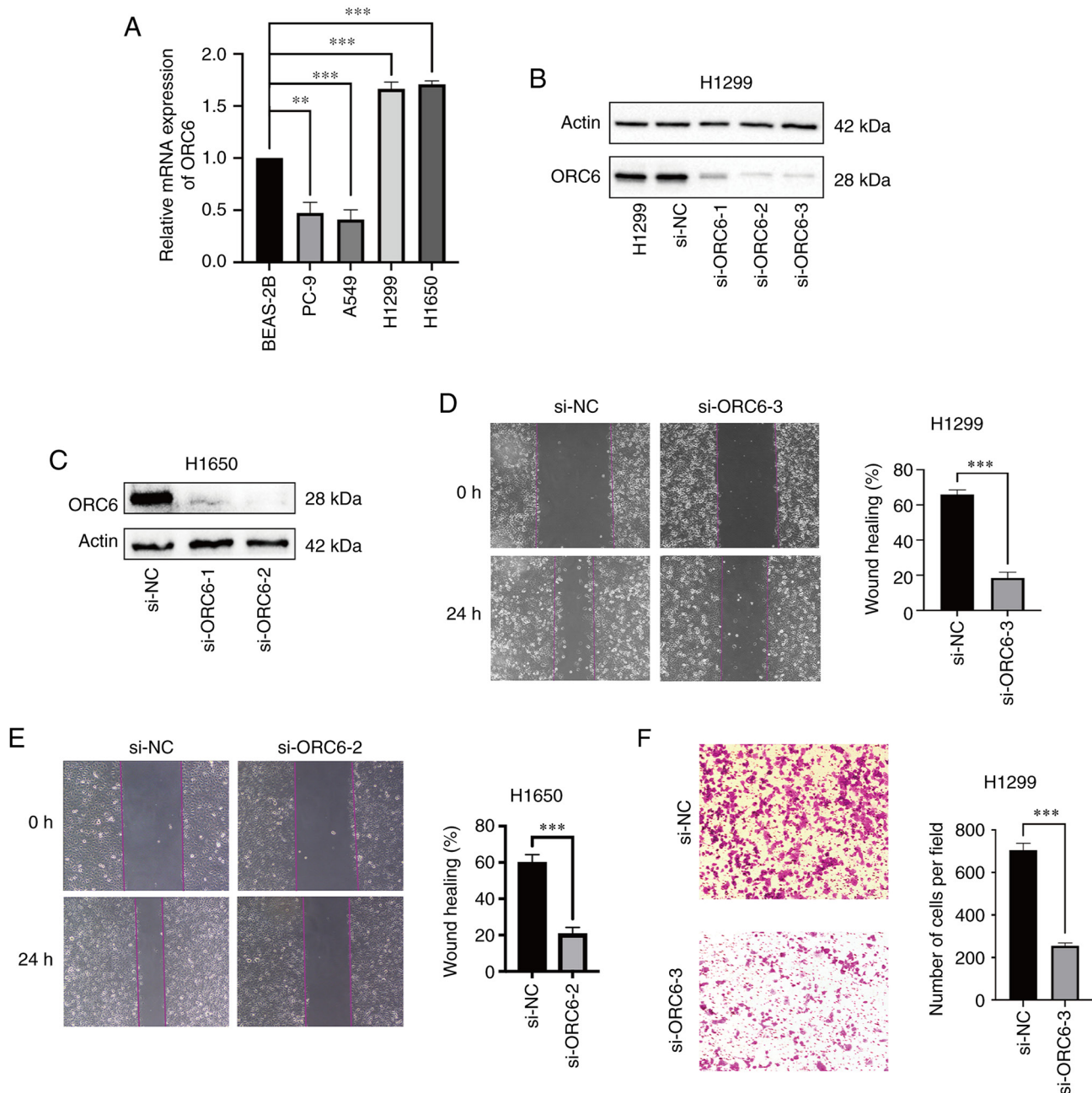


Figure 8. Inhibition of proliferation and migration of lung cancer cells when ORC6 is knocked-down *in vitro*. (A) Expression of ORC6 in five cell lines analyzed using reverse transcription-quantitative PCR. Western blot analysis performed to assess the transfection efficiency of si-NC, si-ORC6-1, si-ORC6-2 and si-ORC6-3 in (B) H1299 and (C) H1650 cells. Wound healing assays demonstrated a delay in wound closure in (D) H1299 and (E) H1650 cells with significantly reduced ORC6 expression, magnification, x100. (F) Transwell migration assay indicated alterations in the migration of H1299 cells following knockdown of ORC6, magnification, x100. ** $P < 0.01$; *** $P < 0.001$. ORC, origin recognition complex; si, small interfering; NC, negative control.

mechanisms of NSCLC, and to identify novel therapeutic biomarkers and targets.

The present study detected altered levels of ORC6 mRNA expression in the majority of tumors, particularly in cases of lung cancer, by analyzing databases such as TCGA. Additionally, RT-qPCR demonstrated the notable increase in ORC6 mRNA expression in lung carcinoma cells. Upregulation of ORC6 in lung carcinoma was associated with certain clinical and pathological factors. However, a significant strong correlation was demonstrated between elevated ORC6 expression and an unfavorable prognosis in patients with NSCLC, compared with that in patients with low expression of ORC6.

Correlation, Cox regression and logistic regression analyses revealed an association between increased ORC6 expression in patients with NSCLC and specific clinical characteristics, including the stage of the disease and the grade of the tumor.

Previous studies have indicated that ORC6 has a tumorigenic function in facilitating the progression of cancer and may potentially function as an adverse indicator for NSCLC (38).

To assess the possible biological roles of genes that are expressed differently, enrichment analyses using GO and KEGG were performed. The findings indicated that these genes were primarily enriched in 'organelle fission', 'nuclear division', 'chromosome segregation', 'mitotic nuclear division' and 'nuclear

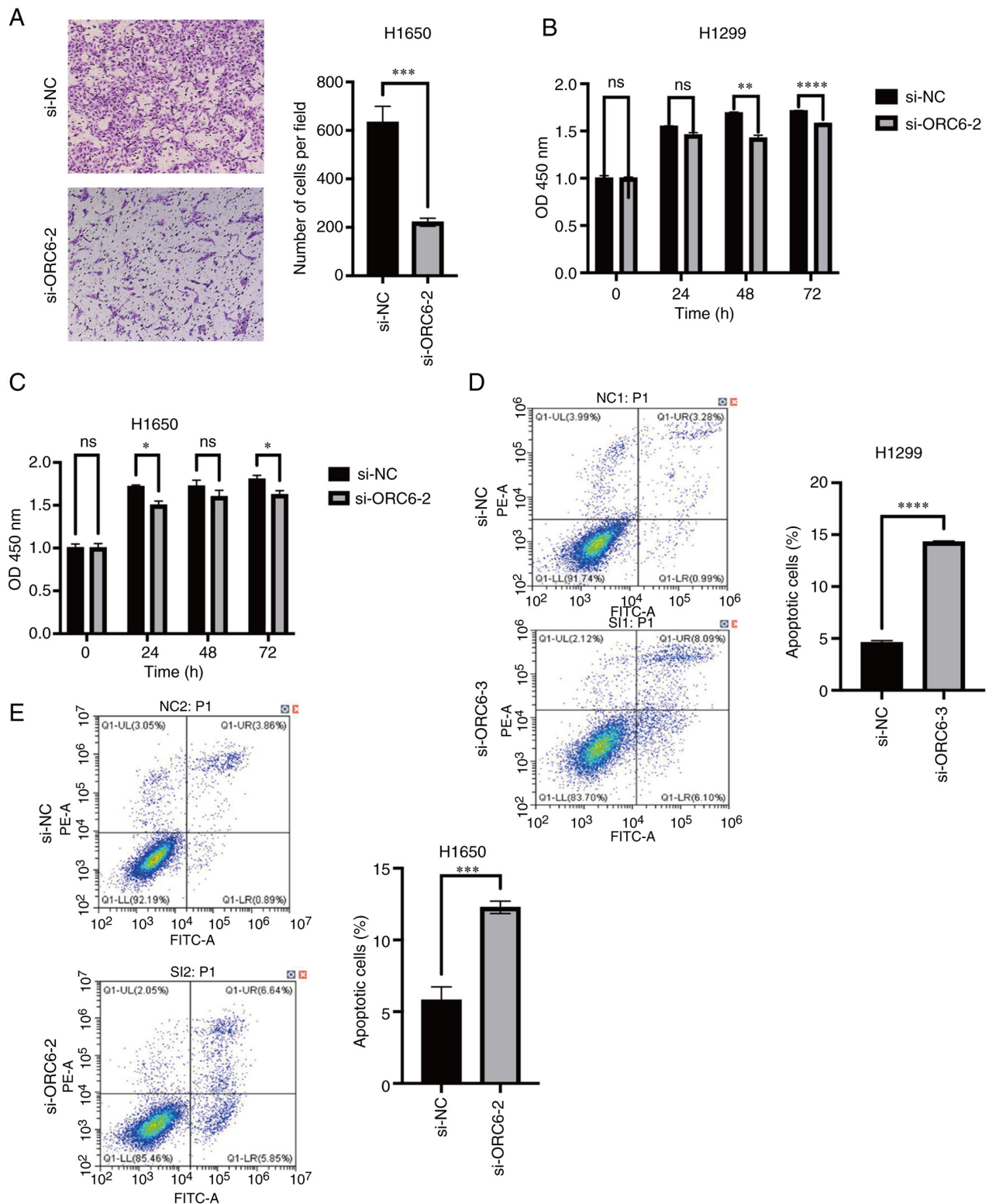


Figure 9. Inhibition of cell proliferation and migration, along with the induction of cell apoptosis, is observed upon *in vitro* knockdown of ORC6. (A) Transwell migration assay indicated alterations in the migration of H1650 cells following knockdown of ORC6 expression, magnification, x100. Silenced ORC6 expression significantly repressed the proliferation of (B) H1299 and (C) H1650 cells. After transfection, apoptosis of (D) H1299 and (E) H1650 cells was measured using flow cytometry. * $P < 0.05$; ** $P < 0.01$; *** $P < 0.001$; **** $P < 0.0001$. ORC, origin recognition complex; si, small interfering; NC, negative control; OD, optical density; ns, not significant.

chromosome separation', which could impact the proliferation of cancer cells, potentially influencing the progression of NSCLC.

A notable finding of the present study was the association between the expression of ORC6 and the TME. In the high

ORC6 expression group, naive B cells, memory resting CD4 T cells, monocytes, resting and activated DCs, and resting mast cells had lower enrichment scores. Conversely, CD8 T, memory-activated CD4 T, follicular helper T and resting

NK cells, as well as M0 and M1 macrophages had higher enrichment scores in the high ORC6 expression group. CD8⁺ T cells and M1 macrophages, as cytotoxic cells, serve a crucial role in orchestrating antitumor immune responses and markedly impact the outcomes of cancer immunotherapy. However, the present study demonstrated that ORC6 could promote the occurrence and development of lung adenocarcinoma. This may be because resting and activated DCs in the ORC6 upregulation group demonstrated lower enrichment scores. DCs are currently known as the most potent type of antigen-presenting cells (APCs) and the only APCs capable of activating naive T lymphocytes, thus holding a central position in the immune response (39). As specialized APCs, DCs serve a crucial role in initiating and regulating both innate and adaptive immune responses, and possess unique abilities to activate (initiate) CD4 T cells (40). In summary, high expression of ORC6 may exacerbate immune escape in tumor cells, leading to the occurrence, development and metastasis of tumors. Therefore, ORC6 may be a potential target for immunotherapy, but further research is needed to verify these findings.

To further assess the function of ORC6 in NSCLC, certain experiments were performed. The results of wound healing and Transwell assays indicated that silencing ORC6 expression significantly reduced the invasive ability of lung cancer cells. CCK-8 assays demonstrated that knock-down of ORC6 expression led to a noticeable decrease in the proliferation of lung cancer cells. The results of the cell apoptosis assay indicated that knock-down of ORC6 expression significantly promoted apoptosis in lung cancer cells. These experimental findings were in-line with the bioinformatics analysis conclusions, and indicated that ORC6 significantly promoted the proliferation, migration and invasion of NSCLC cells whilst inhibiting apoptosis.

To summarize, the present study mainly assessed the association between ORC6 and lung carcinoma using bioinformatics analyses and multiple experiments. The findings suggest that ORC6 can be classified as an oncogene in NSCLC and may be a promising diagnostic biomarker, as its levels of expression have been associated with an increase in the stage and grade of the tumor. These findings may assist clinicians to identify patients with NSCLC who are more likely to experience disease recurrence and resistance to chemotherapy. As a result, more intensive treatment approaches may be suggested for patients who have elevated levels of ORC6 expression.

Despite performing cross-validation with several databases, the present study has certain limitations. Inaccurate data collected in databases could result in biases during data collection. Due to a lack of relevant research, an explanation for why resting and activated DCs in the high ORC6 expression group demonstrated lower enrichment scores cannot be provided. At the experimental level, there were also shortcomings. Due to the lack of assessment of the downstream targets of ORC6, it is unclear how ORC6 regulates cellular functions and signal transduction. Additionally, as a mouse tumor model was not used to evaluate the role of ORC6 in NSCLC, further investigation is needed to understand the biological impact of ORC6 *in vivo*. Furthermore, the absence of experiments involving chemotherapy-related drugs underscores the need to explore the interaction between ORC6 and chemotherapy agents, as well as the potential implications during the treatment process.

These deficiencies highlight the need for further research to deepen our understanding of the mechanistic role of ORC6 and its potential implications in disease treatment.

In conclusion, the present study demonstrated that ORC6 was significantly increased in NSCLC and its overexpression was strongly associated with the clinical advancement of the condition. Moreover, the current study revealed a crucial function for ORC6 in the enhancement of the proliferation and infiltration of NSCLC cells, thus indicating its potential as a tool for diagnosing and predicting the outcome of NSCLC. These findings provide new perspectives on the involvement of ORC6 in the development of NSCLC and may potentially lead to innovative strategies for the detection and treatment of this condition.

Acknowledgements

Not applicable.

Funding

The present study was supported by the National Natural Science Foundation of China (grant nos. 81160294 and 81960425).

Availability of data and materials

The datasets used and/or analyzed during the current study are available from the corresponding author on reasonable request.

Authors' contributions

Study design was performed by JX and LC. Data collection and analysis were performed by DZ, YC, LC, HZ, ZL and ZY. LC, DZ, YC, HZ, ZL, ZY and JX contributed to data interpretation and to the writing and review of this manuscript. JX and LC confirm the authenticity of all the raw data. All authors have read and approved the final manuscript.

Ethics approval and consent to participate

Not applicable.

Patient consent for publication

Not applicable.

Competing interests

The authors declare that they have no competing interests.

References

1. Yang K, Li Z, Chen Y, Yin F, Ji X, Zhou J, Li X, Zeng T, Fei C, Ren C, *et al*: Na, K-ATPase $\alpha 1$ cooperates with its endogenous ligand to reprogram immune microenvironment of lung carcinoma and promotes immune escape. *Sci Adv* 9: eade5393, 2023.
2. Hinterleitner C, Strähle J, Malenke E, Hinterleitner M, Henning M, Seehawer M, Bilich T, Heitmann J, Lutz M, Mattern S, *et al*: Platelet PD-L1 reflects collective intratumoral PD-L1 expression and predicts immunotherapy response in non-small cell lung cancer. *Nat Commun* 12: 7005, 2021.

3. Herbst RS, Baas P, Kim DW, Felip E, Pérez-Gracia JL, Han JY, Molina J, Kim JH, Arvis CD, Ahn MJ, *et al*: Pembrolizumab versus docetaxel for previously treated, PD-L1-positive, advanced non-small-cell lung cancer (KEYNOTE-010): A randomised controlled trial. *Lancet* 387: 1540-1550, 2016.
4. Rittmeyer A, Barlesi F, Waterkamp D, Park K, Ciardiello F, von Pawel J, Gadgeel SM, Hida T, Kowalski DM, Dols MC, *et al*: Atezolizumab versus docetaxel in patients with previously treated non-small-cell lung cancer (OAK): A phase 3, open-label, multicentre randomised controlled trial. *Lancet* 389: 255-265, 2017.
5. Aguiar PN Jr, Santoro IL, Tadokoro H, de Lima Lopes G, Filardi BA, Oliveira P, Mountzios G and de Mello RA: The role of PD-L1 expression as a predictive biomarker in advanced non-small-cell lung cancer: A network meta-analysis. *Immunotherapy* 8: 479-488, 2016.
6. Aguiar PN Jr, De Mello RA, Hall P, Tadokoro H and de Lopes G: PD-L1 expression as a predictive biomarker in advanced non-small-cell lung cancer: Updated survival data. *Immunotherapy* 9: 499-506, 2017.
7. Kim H and Chung JH: PD-L1 Testing in non-small cell lung cancer: Past, present, and future. *J Pathol Transl Med* 54: 196, 2019.
8. Ettinger DS, Wood DE, Aisner DL, Akerley W, Bauman JR, Bharat A, Bruno DS, Chang JY, Chirieac LR, D'Amico TA, *et al*: Non-small cell lung cancer, version 3.2022, NCCN clinical practice guidelines in oncology. *J Natl Compr Canc Netw* 20: 497-530, 2022.
9. Shibata E, Kiran M, Shibata Y, Singh S, Kiran S and Dutta A: Two subunits of human ORC are dispensable for DNA replication and proliferation. *Elife* 5: e19084, 2016.
10. Bell SP, Kobayashi R and Stillman B: Yeast origin recognition complex functions in transcription silencing and DNA replication. *Science* 262: 1844-1849, 1993.
11. Chesnokov IN, Chesnokova ON and Botchan M: A cytokinetic function of Drosophila ORC6 protein resides in a domain distinct from its replication activity. *Proc Natl Acad Sci USA* 100: 9150-9155, 2003.
12. Semple JW, Da-Silva LF, Jervis EJ, Ah-Kee J, Al-Attar H, Kummer L, Heikkilä JJ, Pasero P and Duncker BP: An essential role for Orc6 in DNA replication through maintenance of pre-replicative complexes. *EMBO J* 25: 5150-5158, 2006.
13. Chen S, de Vries MA and Bell SP: Orc6 is required for dynamic recruitment of Cdt1 during repeated Mcm2-7 loading. *Genes Dev* 21: 2897-2907, 2007.
14. Liu S, Balasov M, Wang H, Wu L, Chesnokov IN and Liu Y: Structural analysis of human Orc6 protein reveals a homology with transcription factor TFIIB. *Proc Natl Acad Sci USA* 108: 7373-7378, 2011.
15. Prasanth SG, Prasanth KV and Stillman B: Orc6 involved in DNA replication, chromosome segregation, and cytokinesis. *Science* 297: 1026-1031, 2002.
16. Wang XK, Wang QQ, Huang JL, Zhang LB, Zhou X, Liu JQ, Chen ZJ, Liao XW, Huang R, Yang CK, *et al*: Novel candidate biomarkers of origin recognition complex 1, 5 and 6 for survival surveillance in patients with hepatocellular carcinoma. *J Cancer* 11: 1869-1882, 2020.
17. Pan Q, Li F, Ding Y, Huang H and Guo J: ORC6 acts as a biomarker and reflects poor outcome in clear cell renal cell carcinoma. *J Cancer* 13: 2504-2514, 2022.
18. Senter NC, McCulley A, Kuznetsov VA and Feng W: Identification of recurrent chromosome breaks underlying structural rearrangements in mammary cancer cell lines. *Genes (Basel)* 13: 1228, 2022.
19. Hu Y, Wang L, Li Z, Wan Z, Shao M, Wu S and Wang G: Potential prognostic and diagnostic values of CDC6, CDC45, ORC6 and SNHG7 in colorectal cancer. *Onco Targets Ther* 12: 11609-11621, 2019.
20. Wei J, Yin Y, Deng Q, Zhou J, Wang Y, Yin G, Yang J and Tang Y: Integrative analysis of MicroRNA and gene interactions for revealing candidate signatures in prostate cancer. *Front Genet* 11: 176, 2020.
21. Liu Y, Chen P, Li M, Fei H, Huang J, Zhao T and Li T: Comprehensive analysis of the control of cancer stem cell characteristics in endometrial cancer by network analysis. *Comput Math Methods Med* 2021: 6653295, 2021.
22. Wang Z, Jensen MA and Zenklusen JC: A practical guide to the cancer genome atlas (TCGA). *Methods Mol Biol* 1418: 111-141, 2016.
23. In J and Lee DK: Survival analysis: Part II-applied clinical data analysis. *Korean J Anesthesiol* 76: 84-85, 2019.
24. Ritchie ME, Phipson B, Wu D, Hu Y, Law CW, Shi W and Smyth GK: limma powers differential expression analyses for RNA-sequencing and microarray studies. *Nucleic Acids Res* 43: e47, 2015.
25. Chen B, Khodadoust MS, Liu CL, Newman AM and Alizadeh AA: Profiling tumor infiltrating immune cells with CIBERSORT. *Methods Mol Biol* 1711: 243-259, 2018.
26. Hänzelmann S, Castelo R and Guinney J: GSVA: Gene set variation analysis for microarray and RNA-seq data. *BMC Bioinformatics* 14: 7, 2013.
27. Livak KJ and Schmittgen TD: Analysis of relative gene expression data using real-time quantitative PCR and the 2(-Delta Delta C(T)) method. *Methods* 25: 402-408, 2001.
28. Li T, Fu J, Zeng Z, Cohen D, Li J, Chen Q, Li B and Liu XS: TIMER2.0 for analysis of tumor-infiltrating immune cells. *Nucleic Acids Res* 48: W509-W514, 2020.
29. Hayford CE, Tyson DR, Robbins CJ III, Frick PL, Quaranta V and Harris LA: An in vitro model of tumor heterogeneity resolves genetic, epigenetic, and stochastic sources of cell state variability. *PLoS Biol* 19: e3000797, 2021.
30. Xu N, You Y, Liu C, Balasov M, Lun LT, Geng Y, Fung CP, Miao H, Tian H, Choy TT, *et al*: Structural basis of DNA replication origin recognition by human Orc6 protein binding with DNA. *Nucleic Acids Res* 48: 11146-11161, 2020.
31. Bleichert F, Botchan MR and Berger JM: Crystal structure of the eukaryotic origin recognition complex. *Nature* 519: 321-326, 2015.
32. Balasov M, Huijbregts RP and Chesnokov I: Role of the Orc6 protein in origin recognition complex-dependent DNA binding and replication in Drosophila melanogaster. *Mol Cell Biol* 27: 3143-3153, 2007.
33. Thomae AW, Baltin J, Pich D, Deutsch MJ, Ravasz M, Zeller K, Gossen M, Hammerschmidt W and Schepers A: Different roles of the human Orc6 protein in the replication initiation process. *Cell Mol Life Sci* 68: 3741-3756, 2011.
34. Siegel RL, Miller KD, Wagle NS and Jemal A: Cancer statistics, 2023. *CA Cancer J Clin* 73: 17-48, 2023.
35. Sung H, Ferlay J, Siegel RL, Laversanne M, Soerjomataram I, Jemal A and Bray F: Global cancer statistics 2020: GLOBOCAN estimates of incidence and mortality worldwide for 36 cancers in 185 countries. *CA Cancer J Clin* 71: 209-249, 2021.
36. Kumar M and Sarkar A: Current therapeutic strategies and challenges in nscLc treatment: A comprehensive review. *Exp Oncol* 44: 7-16, 2022.
37. He D, Wang D, Lu P, Yang N, Xue Z, Zhu X, Zhang P and Fan G: Single-cell RNA sequencing reveals heterogeneous tumor and immune cell populations in early-stage lung adenocarcinomas harboring EGFR mutations. *Oncogene* 40: 355-368, 2021.
38. Tang M, Chen J, Zeng T, Ye DM, Li YK, Zou J and Zhang YP: Systemic analysis of the DNA replication regulator origin recognition complex in lung adenocarcinomas identifies prognostic and expression significance. *Cancer Med* 12: 5035-5054, 2023.
39. Gilboa E: DC-based cancer vaccines. *J Clin Invest* 117: 1195-1203, 2007.
40. Steinman RM: Decisions about dendritic cells: Past, present, and future. *Annu Rev Immunol* 30: 1-22, 2012.



Copyright © 2024 Chen et al. This work is licensed under a Creative Commons Attribution-NonCommercial-NoDerivatives 4.0 International (CC BY-NC-ND 4.0) License.